CRYOGENIC HYDROGEN JETS: FLAMMABLE ENVELOPE SIZE AND HAZARD DISTANCES FOR JET FIRE

Cirrone, D., Makarov, D. and Molkov, V.
[1]Hydrogen Safety Engineering and Research Centre (HySAFER),
Ulster University, Shore Road, Newtownabbey, BT37 0QB, UK,
d.cirrone@ulster.ac.uk, dv.makarov@ulster.ac.uk, v.molkov@ulster.ac.uk

ABSTRACT

Engineering tools for calculation of hazard distances for cryogenic hydrogen jets are currently missing. This study aims at the development of validated correlations for calculation of hazard distances for cryogenic unignited releases and jet fires. The experiments performed by Sandia National Laboratories (SNL) on jets from storage temperature in the range 46-295 K and pressure up to 6 bar abs are used to expand the validation domain of the correlations. The Ulster's under-expanded jet theory is applied to calculate parameters at the real nozzle exit. The similarity law for concentration decay in momentum-dominated jets is shown to be capable to reproduce experimental data of SNL on 9 unignited cryogenic releases. The accuracy of the similarity law to predict experimentally measured axial concentration decay improves with the increase of the release diameter. This is thought due to decrease of the effect of friction and minor losses for large release orifices. The dimensionless flame length correlation is applied to analyse 30 cryogenic jet fire tests. The deviation of calculated flame length from measured in experiments is mostly within acceptable accuracy for engineering correlations, 20%, similarly to releases from storage and equipment at atmospheric temperatures. It is concluded that the similarity law and the dimensionless flame correlation can be used as universal engineering tools for calculation of hazard distances for hydrogen releases at any storage temperature, including cryogenic.

1. INTRODUCTION

The necessity of high storage capacities, such as for large fuelling stations (>400 kg/day) or transport trailers (~3500 kg of LH_2/trailer) [1], has led to the employment of super-insulated vessels storing hydrogen as cryo-compressed or liquid. Considering a cryogenic vessel with pressure equal to 10 bar, the storage density increases from 0.83 kg/m^3 to 1.61 kg/m^3 for a decrease of temperature from 288 K to 150 K [2]. Values up to 7.28 kg/m^3 are reached for temperature down to 40 K. Density increases even further if hydrogen is stored as a liquid, reaching 71 kg/m^3 at the boiling point conditions, i.e. ambient pressure and temperature equal to 20 K. Despite a well-known advantage in volumetric capacity, there is not yet a full understanding of the hazards from cryogenic releases of hydrogen, and validated predictive tools to be used in hydrogen safety engineering are currently missing. The major risk related to unignited gaseous jets is the formation of a flammable hydrogen-air cloud, which constitutes a serious danger of jet fires, deflagration and detonation. Thus, it is of primary interest to have a tool able to evaluate the distances where flammable hydrogen concentration in air is present. Friedrich et al.'s performed experiments on hydrogen releases with pressures from 7 to 35 bar abs and temperature in the range 34-65 K [3]. The authors observed that hydrogen concentration decays "slower" than in warm jets. These tests along with other liquefied (LH_2) and cryo-compressed hydrogen unignited jets were investigated numerically in [4]–[6]. The studies conducted in Sandia National Laboratories (SNL) in USA on hydrogen releases with pressure 2-5 bar abs and temperature 50-61 K led to a concentration decay similar to room temperature releases [7]. The similarity law for concentration decay in momentum-dominated expanded jets [8] was validated for under-expanded jets with release temperature down to 80 K and pressure in the range 2.6–400 bar if density in the real nozzle is calculated using Ulster's under-expanded jet theory [9]. In the present study the similarity law is applied to releases with temperature as low as 50 K (9 experiments on hydrogen unignited jets

performed at SNL [7]). Experiments by Friedrich et al.'s included also ignition of the cryogenic hydrogen jets, to analyse the flame stability, combustion regimes and thermal radiation of cryogenic jet fires. In 2017 the SNL conducted experiments on cryogenic hydrogen jet fires with release temperature 37-295 K and pressures up to 6 bar abs [10]. In their study the flame length was found to correlate well with the square root of the Reynolds number. In 2013 the dimensionless correlation for hydrogen jet flames was developed at Ulster [11]. It accounts not only for Reynolds number but Mach and Froude numbers too. The correlation was validated against jet fires with pressure in the range 10-900 bar and temperature in the range 187-300 K. The present study aims at analysing the performance of the mentioned correlations, i.e. the similarity law for hydrogen concentration decay in momentum-dominated unignited jet and the dimensionless correlation for hydrogen jet fires, when they are applied to releases from a storage with low temperature down to 46 K.

2. DESCRIPTION OF EXPERIMENTS

The experiments were conducted at the Turbulent Combustion Laboratory of SNL in USA [10], [7]. The release temperature and pressure were maintained constant during each test and monitored upstream the interchangeable orifice of diameter 0.75 mm or 1 mm or 1.25 mm. The hydrogen was released vertically upward in the laboratory equipped with an exhaust gases collection system. The exhaust hood volumetric flow rate was changed based on the test typology (ignited or unignited) and the hydrogen mass flow rate.

Unignited releases

The scope of the experiments on unignited releases was to characterise the jets in terms of hydrogen concentration and temperature distribution. Release temperature and pressure were included in the range 50-61 K and 2-5 bar abs respectively. Details of the release conditions for each test are given in Table 1. A co-flow of air through a 19 cm diameter honeycomb with velocity 0.3 m/s surrounded the jet. The exhaust gases volumetric flow rate was typically 6 m^3/h. Hydrogen concentration was determined through the Raman scattering technique. The laser covered an area with 10 mm length. Therefore, the release point was moved axially so that the laser system could measure the concentration in each 10 mm portion of the jet up to 100 mm from the release point. Each measurement is given by the average of 400 laser pulses. Temperature distribution in the jet was calculated by experimentalists from the measured concentration using the ideal gas law. The authors reported that this could lead to an error of nearly 10% for low temperatures, whereas it decreases to 1% for temperatures above 50 K. Additional to publication [7] experimental data were provided by the authors of [7] through personal communication.

Table 1. Experimental operating conditions of 9 validation unignited tests [7].

Test No.	d, mm	Temperature, K	Pressure, bar abs
1	1.00	58	2.0
2	1.00	56	3.0
3	1.00	53	4.0
4	1.00	50	5.0
5	1.25	61	2.0
6	1.25	51	2.5
7	1.25	51	3.0
8	1.25	55	3.5
9	1.25	54	4.0

Ignited releases (jet fires)

The scope of the ignited releases tests was to investigate the ignition and flame characteristics of cryogenic under-expanded jet fires. Release temperature and pressure were included in the ranges 46-

295 K and 2-6 bar abs respectively. The exhaust hood volumetric flow rate was varied from approximately 5100 to 7650 m^3/h, depending on the hydrogen mass flow rate. The flame length was given as average of the visible and infrared (IR) cameras images. Experiments included measurements of the radiative heat flux in the surroundings of the jet fires. A selection of 30 tests was used for the model validation of the present study. Additional to publication [10] experimental data were provided by the authors of [10] through personal communication.

3. RELEASE SOURCE MODELLING

Experiments operated at pressure up to 6 bar abs. At release pressures above 2 bar abs an under-expanded jet is expected, as pressure at the nozzle exit is above atmospheric. The under-expanded jet theory [12] is employed to calculate the flow parameters, i.e. density and velocity, at the real (actual) nozzle exit required by the similarity law and by the dimensionless flame length correlation. The approach employs the Abel-Noble Equation of State (EOS) to describe the non-ideal behaviour of the gas at low temperatures. Release conditions are calculated assuming chocked flow at the nozzle, isentropic expansion and conservation of energy between the stagnation and release locations.

The temperature and pressure measured in the release pipe before the orifice are assumed as at stagnation conditions (indicated with subscript 0). However, flow velocity in the pipe section upstream the release point, u_0, is not equal to 0. Therefore, it is needed to verify that the associated dynamic pressure, $\rho_0 u_0^2/2$, is negligible compared to the measured static pressure to prove the validity of stagnation conditions assumptions. The diameter of the release pipe is equal to 10.2 mm, whereas the nozzle openings are 1.00 and 1.25 mm in diameter. Using the conservation of mass between the pipe and the orifice, it is possible to calculate the velocity of the flow in the larger section pipe (d=10.2 mm). Dynamic pressure resulted to be less than 0.01% of the static pressure, confirming that it can be neglected, and stagnation assumption be used.

Previous study in [13] showed that Ulster's under-expanded jet theory estimated well the experimental mass flow rate for 30 tests reported in [10] and [14]. In the present study, calculations were expanded to further 81 tests [15]-[16]. In 77 tests, indicated as d=1.00 mm* in Figure 1, out of the additional 81 tests release temperature was retrieved graphically from a chromatic legend [15] and not from exact values. The authors estimate that the inaccuracy in the release temperature approximation is maximum ±10K. Such inaccuracy in temperature can lead up to 10% relative difference in the mass flow rate calculation for the lowest release temperature (37 K). The relative difference is observed to decrease with the increase of release temperature to 7% and 5% for T=65 K and T=95 K respectively. Comparison between calculated mass flow rate against experiments is given in Figure 1. Deviation from experiments is contained within ±10% with the exception of a test with T=37 K and P=2 bar abs (deviation 23%). This test may be affected by the accuracy in retrieving graphically the release temperature. Following the general good agreement between calculated mass flow rate and experiments, it is concluded that the under-expanded jet theory can be used to calculate the flow conditions at the nozzle exit to be used in the following sections.

A second evaluation compared Abel-Noble EOS performance to that of NIST EOS [2], which is generally employed to model LH_2 and cryogenic hydrogen release sources [4]–[6]. Previous study in [13] showed that Abel-Noble EOS can be applied to gaseous releases at cryogenic temperatures for pressure up to 6 bar abs, given that a negligible difference was observed between the density calculated using the two EOSs. In the present study the mass flow rate calculated using the under-expanded jet theory and Abel Noble EOS is compared to the mass flow rate evaluated employing NIST EOS for normal hydrogen. The latter EOS is based on the explicit modelling of the Helmotz free energy. The entropy and enthalpy at the storage conditions, s_0 and h_0 respectively, were determined from the stagnation temperature and pressure, given that the fluid is in single-phase conditions. The exit conditions were iteratively calculated gradually decreasing temperature along the isentropic expansion transformation from the "storage" conditions $s(T,P) = s_0(T_0,P_0)$, until the equation of energy conservation between storage and exit nozzle was satisfied with a tolerance of 10 J/kg:

$$h_n - h_0 + \frac{u_n^2}{2} = 0 \quad (1)$$

Enthalpy, h_n, and speed of sound, u_n, at the exit nozzle were determined by the NIST EOS. Conditions at the exit nozzle were all located in the gaseous phase. Therefore, they do not necessitate further considerations or expressions to determine the flow properties. This procedure was applied to the 39 unignited and ignited tests investigated through the similarity law and the dimensionless flame length correlation. It is found that the maximum variation in the mass flow rate calculated with NIST EOS is 7% and it is given, as expected, for the release at the lowest temperature (46 K). Therefore, it is confirmed that for pressures up to 6 bar abs, the two EOSs can be used interchangeably without affecting significantly the resulting release mass flow rate.

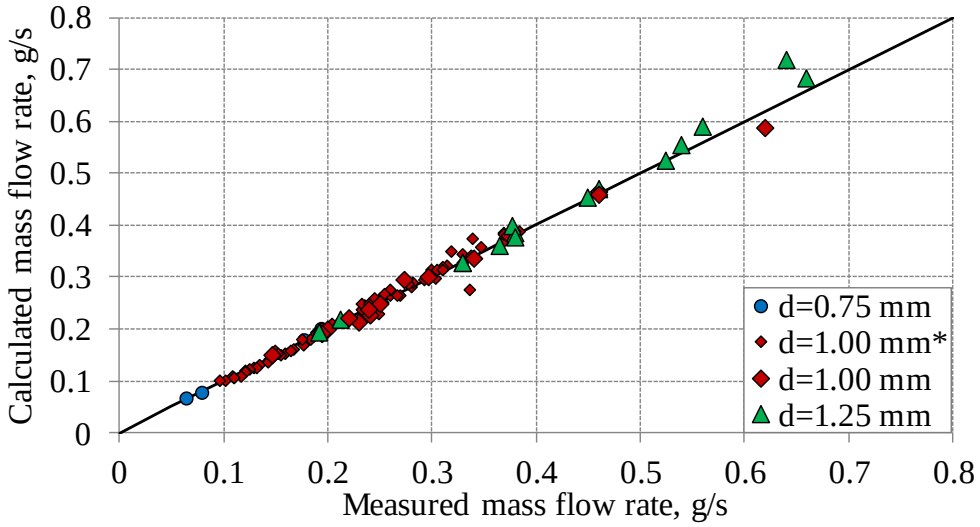

Figure 1. Calculated versus experimental mass flow rate

4. CRYOGENIC UNIGNITED JETS

4.1. The similarity law for concentration decay in momentum-dominated jets

The similarity law for expanded and under-expanded jets [8] is employed here to calculate axial hydrogen concentration decay in cryogenic momentum-controlled jets:

$$C_{ax} = 5.4 \sqrt{\frac{\rho_N}{\rho_s}} \frac{d}{x}, \quad (2)$$

where ρ_N is the density of hydrogen at the nozzle, ρ_s is the density of the surrounding air, d is the nozzle diameter and x is the distance from the release point. Once a concentration of interest is defined, it is possible to calculate the distance from the nozzle where this is reached. For instance, the similarity law allows to calculate the location at which the Lower Flammability Limit (LFL) is reached (4%) to determine the axial size of the flammable envelope produced by an unintended hydrogen release.

Prior to applying the similarity law, it was verified that the jets are momentum controlled. The Froude number was calculated as:

$$Fr = \frac{u_N^2}{gd}, \quad (3)$$

where u_N is the velocity at the nozzle and g is the gravity acceleration. The logarithm of Froude number for all the tests is above 7, meaning that all the investigated jets are momentum controlled at least up to the distance where hydrogen concentration 4% is reached [17].

4.2. Results and discussion

The mass flow rate was measured during the experiments. However, only results for 1 mm diameter releases were considered reliable by the experimentalists, whereas results for 1.25 mm could have been affected by significant inaccuracy [16]. Therefore, calculated mass flow rate is compared against the 4 unignited tests with d=1 mm, predicting experimental results within ±6% accuracy. The tests are included in Figure 1.

The hydrogen concentration decay calculated from the similarity law is compared against experiments in Figure 2. The similarity law well represents hydrogen concentration decay for releases through the 1.25 mm diameter nozzle. Maximum deviation is 10% and it is given for the release at 2 bar abs. Deviation decreases to below 5% for the jets with release pressure above 2 bar, providing an excellent agreement between experiments and calculations. Predictions worsen for the releases with diameter 1 mm. It must be noted that experimental measurements have a more unstable concentration decay along the axis, showing significant discontinuities in the joining points of the 10 mm measurements slots of the laser. As a result of these instabilities, it is observed that the similarity law may result in under or overpredictions in different portions of the jet axis. Concentration decay for test 4 (T=50 K and P=5 bar abs) results to be well reproduced along the axis within a 6-9 cm distance, whereas it is underestimated outside this range. Although these instabilities, concentration is yet reasonably predicted for tests 1 and 4, characterised by the lowest and highest pressures, respectively 2 and 5 bar abs. Predictions show a deviation for the remaining two tests, arriving up to 25% for test 3 (T=53 K and P=4 bar abs). These two experimental tests show an anomalous behaviour. Test 2 has release pressure higher than test 1, whereas its release temperature is lower. Thus, it is expected that hydrogen concentration along the jet in test 2 would be higher than test 1. Experimental results showed the opposite situation. Similar behaviour was observed for test 3. Hydrogen concentration in test 3 resulted to be lower than test 2 up to 5 cm distance from the nozzle exit, regardless the higher pressure and lower temperature at the release. Reasons for these experimental results may be due to several factors. Experimentalists observed the formation of ice near the nozzle, which could likely be the cause of a lateral displacement of the location of maximum hydrogen concentration from the jet axis. Furthermore, losses generally increase for smaller diameter releases. In addition, a smaller orifice could be characterised by a different heat exchange at the nozzle. These could be the causes for a poorer prediction of the tests with orifice 1 mm.

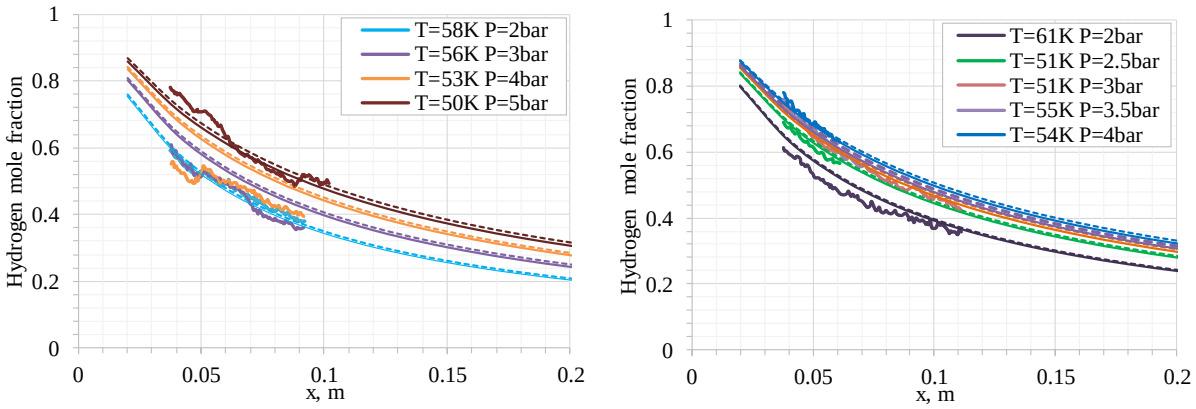

Figure 2. The similarity law estimations using Abel-Noble EOS (thin solid lines) and NIST EOS (dashed lines) against experiments (thick solid lines) for d=1.00 mm (left) and d=1.25 mm (right)

Figure 3 shows the comparison between SNL experimental data and the similarity law. Figure 3 includes as well the experimental data reported in [9] and previously used for validation. Overall, it is showed that the similarity law for axial concentration decay represent well the experiments performed in SNL. Therefore, it can be concluded that the similarity law application can be expanded to temperature down to 50 K for release pressure up to 6 bar abs. The similarity law was used to determine the axial location where concentration decays to 4% in the tests. Distance to LFL increases from 1.22 m to 2.06 m for respectively lowest and highest pressure in case of diameter equal to 1.00 mm. For the 1.25 mm orifice, the distance to LFL slightly increases to 2.25 m. The results obtained using Abel Noble EOS in the under-expanded jet theory are compared to calculations using NIST EOS (dashed lines) in Figure 2. The use of NIST EOS results in a maximum increase of density at the nozzle exit equal to 9% for the release with highest pressure (6 bar abs) and lowest temperature (50 K). The effect is attenuated to 3% variation in the hydrogen concentration decay, due to the square root of density. The analysis is expanded to the distance where concentration equal to ½ LFL is reached (4.5 m), and it is calculated that the difference in hydrogen concentration is maximum 4.5%.

In conclusion, it is observed that the similarity law for concentration decay well reproduces the experimental data for the 9 unignited cryogenic release tests performed in SNL. Therefore, it can be used as an engineering tool to calculate distances to hazardous hydrogen concentration for cryogenic unignited jets down to 50 K release temperature and pressure up to 5 bar abs. Furthermore, it is showed that for the range of pressure 2-5 bar abs and T=50-61 K there is a limited effect of the used real gas EOS on the hydrogen concentration decay.

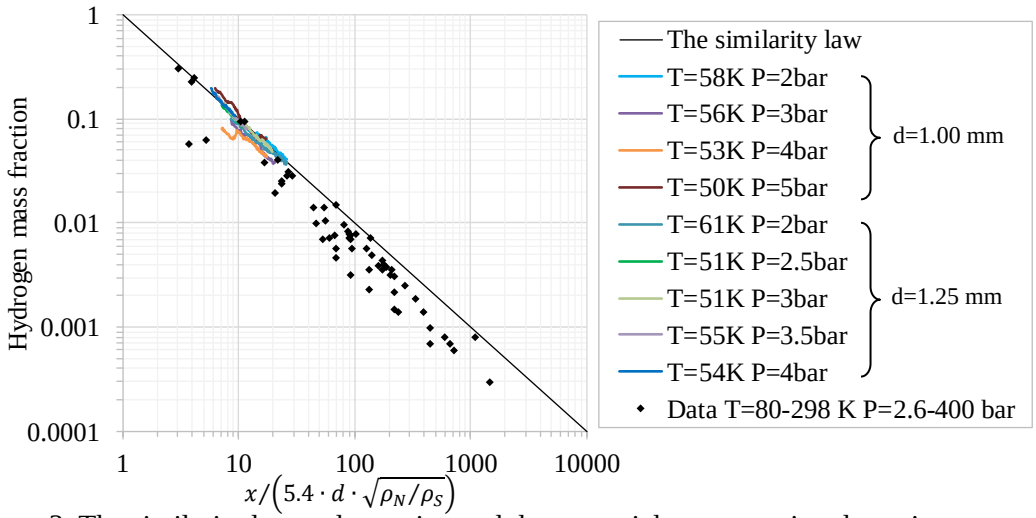

Figure 3. The similarity law and experimental data on axial concentration decay in momentum controlled expanded and under-expanded jets from SNL tests and [9]

5. CRYOGENIC JET FIRES

The dimensionless correlation for hydrogen jet flames developed in [11] was validated against jet fires with pressure in the range 10-900 bar and temperature in the range 187-300 K. Figure 4 shows the dimensionless correlation and experimental data on visible flame length collected in [17]. In the present study, the correlation is applied to SNL tests with release temperature in the range 46 - 295 K to analyse the performance of the model for cryogenic jet fires and expand the correlation validation range. Density and velocity at the nozzle exit are calculated through Ulster's under-expanded jet theory and Abel-Noble EOS. Experimental flame lengths in SNL tests are given as average between visible and infrared measurements. Schefer et al. investigated the flame length using infrared (IR) images, finding out that the IR flame length is longer than the visible flame length: $L_{vis} = 0.88\, L_{IR}$ [18]. This correlation is used to retrieve the visible flame length in SNL tests and report the results in Figure 4. All tests are located in the momentum dominated under-expanded jet region. It is showed that the flame correlation represents conservatively SNL cryogenic jet fires. Three tests with release

pressure equal to 2 bar abs present an exception out of the set of 30 tests, showing an underestimation of the flame length up to 14%.

Temperature at the release is found to greatly affect the resulting flame length. Considering as an example two releases with pressure 2 bar abs and nozzle diameter 1.25 mm, the decrease of temperature from 185 K to 46 K leads to an increase in calculated flame length from 0.40 m to 0.77 m. As a consequence, the minimum distance to not be harmed by the jet fires should increase from 1.4 m to 2.7 m. Calculation of "no harm" distance follows the study in [11], that related the jet fires flame length and temperature distribution along the axis. It was found that the temperature of 70 ºC, which corresponds to a "no harm" criteria for any exposure duration, is achieved at $x = 3.5L_f$.

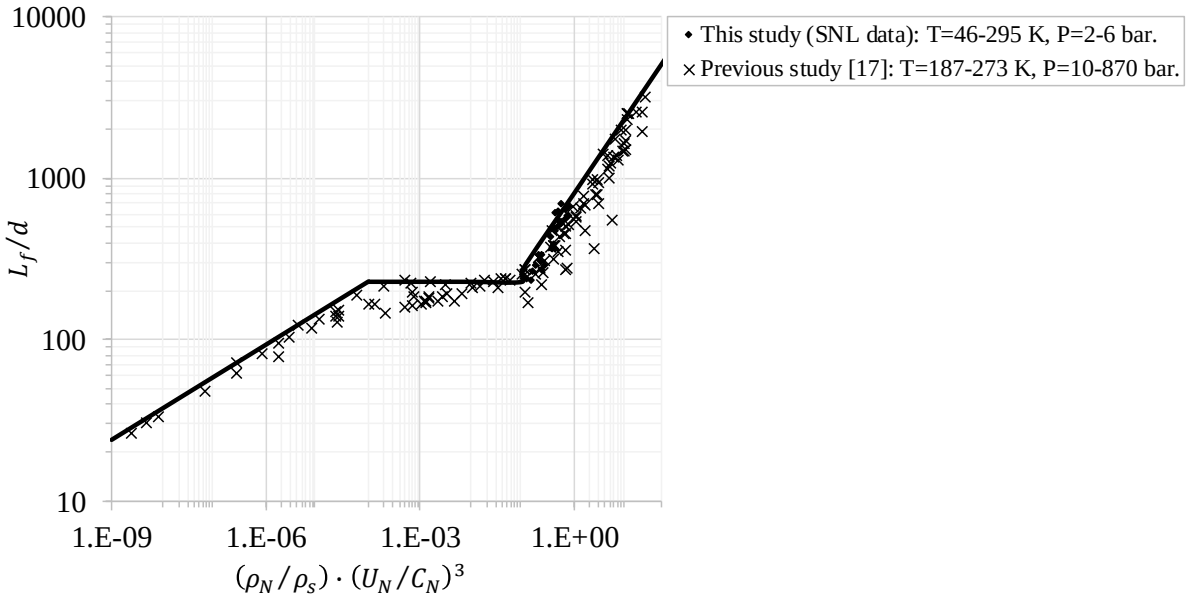

Figure 4. The dimensionless correlation for hydrogen jet flames against experiments: Abel-Noble EOS

The use of NIST EOS in the under-expanded jet theory causes an increase of density at the nozzle exit. The resulting dimensionless parameter $X = (\rho_N/\rho_s)\cdot(U_N/C_N)^3$ is up to 5% larger than the one calculated using Abel-Noble EOS. Figure 5 shows the experimental visible flame length normalised to the nozzle diameter as function of the dimensionless number X with flow conditions calculated using NIST EOS. As well as showed for Abel Noble EOS, the flame correlation represents conservatively SNL cryogenic jet fires with the exception of three tests with release pressure equal to 2 bar abs. Images of the flame length for one of these releases are showed in [10] (T=55 K, P=2 bar abs). The image of the visible flame length has a scale equal to 0.45 m, whereas the image from the infrared camera has a scale of 0.60 m. These lengths are shorter than the average flame length provided in the experimental data (0.66 m). This deviation may be due to the determination of the flame length in experiments as the distance from the nozzle where the intensity drops to 10% of the maximum recorded for that image.

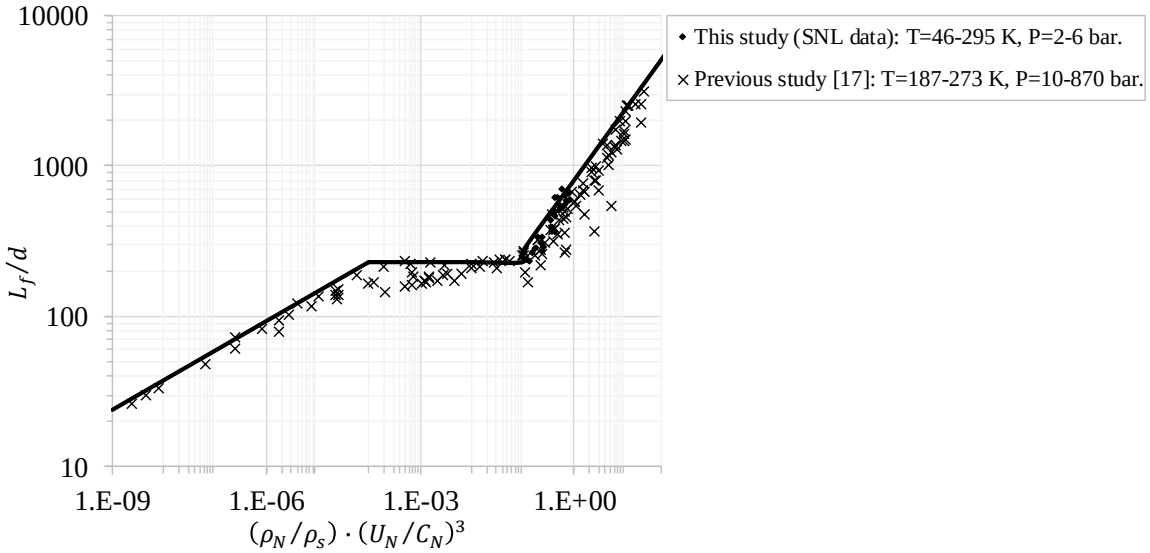

Figure 5. The dimensionless correlation for hydrogen jet flames against experiments: NIST EOS

6. CONCLUSIONS

The Ulster's under-expanded jet theory is found to well represent the mass flow rate of over 100 tests conducted at SNL on cryogenic unignited and ignited jets from storage temperature in the range 46-295 K and pressure up to 6 bar abs. The effect of the equation of state employed to model the non-ideal behaviour of the gas is analysed. The use of NIST EOS or Abel-Noble EOS is found to have a negligible effect for pressures up to 6 bar abs, with a variation of calculated mass flow rate within 7% (coldest jet T=46 K). The originality of the study is given by the extension of applicability of engineering tools previously validated for releases at ambient temperature to cryogenic releases. Approximately 40 experimental tests on cryogenic unignited and ignited releases were used for the validation of the engineering correlations, establishing the rigour of the study. The similarity law for concentration decay in momentum-dominated jets is showed to well reproduce experimental data of SNL for 9 unignited cryogenic releases. The accuracy of the similarity law to reproduce experimentally measured axial concentration decay improves with the increase of the release diameter. It is observed that the effect of the EOS on the calculated concentration decay is negligible. The dimensionless flame correlation for hydrogen jet fires is used to calculate the flame length for 30 cryogenic jet fire tests performed at SNL. The results are found to reproduce experimental flame lengths with an accuracy similar to releases at atmospheric temperatures. The significance of the study is given by the demonstration that the similarity law and the dimensionless flame length correlation can be used as engineering tools for calculation of hazard distances for hydrogen releases at different temperatures, including cryogenic.

ACKNOWLEDGEMENTS

The authors are grateful to Dr P.P. Panda and Dr E. S. Hecht for providing experimental data indispensable to conduct the study. This research has received funding from the Fuel Cells and Hydrogen 2 Joint Undertaking under grant agreement No 779613 (PRESLHY) and No 736648 (NET-Tools). This Joint Undertaking receives support from the European Union's Horizon 2020 research and innovation programme, Hydrogen Europe and Hydrogen Europe research.

REFERENCES

[1] Kunze, K. and Kircher, O., Cryo-Compressed Hydrogen Storage, in Cryogenic Cluster Day, 2012.

[2] Leachman, J.W., Jacobsen, R.T., Lemmon, E.W., Fundamental Equations of State for Parahydrogen, Normal Hydrogen, and Orthohydrogen, J. Phys. Chem. Ref. Data, Vol. 38, no. 3, 2009.
[3] Friedrich, A. et al., Ignition and Heat Radiation of Cryogenic Hydrogen Jets, International Journal of Hydrogen Energy, vol. 37, no. 22, 2012, pp. 17589–17598.
[4] Venetsanos, A.G. and Giannissi, S. G., Release and Dispersion Modeling of Cryogenic Under-expanded Hydrogen Jets, International Journal of Hydrogen Energy, 2016, pp. 1–11.
[5] Giannissi, S. G., Venetsanos, A. G., Markatos, N. and J. G. Bartzis, J. G., CFD Modeling of Hydrogen Dispersion under Cryogenic Release Conditions, International Journal of Hydrogen Energy, vol. 39, no. 28, 2014, pp. 15851–15863.
[6] Venetsanos, A. and Bartzis, J., CFD Modeling of Large-Scale LH2 Spills in Open Environment, International Journal of Hydrogen Energy, vol. 32, no. 13, 2007, pp. 2171–2177.
[7] Hecht, E. S. and Panda, P. P., Mixing and Warming of Cryogenic Hydrogen Releases, International Journal of Hydrogen Energy, 2018, pp. 1–11.
[8] Chen, C. and Rodi, W., Vertical Turbulent Buoyant Jets - a review of experimental data. 1980, Pergamon Press, Oxford.
[9] Saffers, J. B. and Molkov, V. V., Towards Hydrogen Safety Engineering for Reacting and non-Reacting Hydrogen Releases, Journal of Loss Prevention in the Process Industries, vol. 26, no. 2, 2013, pp. 344–350.
[10] Panda, P. P. and Hecht, E. S., Ignition and Flame Characteristics of Cryogenic Hydrogen Releases, International Journal of Hydrogen Energy, vol. 42, no. 1, 2017, pp. 775–785.
[11] Molkov, V. and Saffers, J. B., Hydrogen Jet Flames, International Journal of Hydrogen Energy, vol. 38, no. 19, 2013, pp. 8141–8158.
[12] Molkov, V., Makarov, D. and Bragin, M. V., Physics and Modelling of Underexpanded Jets and Hydrogen Dispersion in Atmosphere, Physics of Extreme States of Matter, 2009, pp. 146–149.
[13] Cirrone, D. M. C., D. Makarov, D. and Molkov, V., Thermal Radiation from Cryogenic Hydrogen Jet Fires, International Journal of Hydrogen Energy, vol. 44, no. 17, 2018, pp. 8874–8885.
[14] Panda, P. P., Private Communication, Sandia National Laboratories, 2016.
[15] Hecht E. S. and Panda, P., R&D for Safety, Codes and Standards: Hydrogen Behavior, 2016.
[16] Hecht, E. S., Private Communication, Sandia National Laboratories, 2019.
[17] Molkov, V., Fundamentals of Hydrogen Safety Engineering I, Free-download electronic book available at www.bookboon.com, 2012.Download free books at bookboon.com, 2012.
[18] Schefer, R. W., Houf, W. G., Bourne, B. and Colton, J., Spatial and Radiative Properties of an Open-Flame Hydrogen Plume, International Journal of Hydrogen Energy, vol. 31, no. 10, 2006, pp. 1332–1340.